

The Structure of Agglomerates Consisting of Polydisperse Particles

M.L. Eggersdorfer and S.E. Pratsinis*

Swiss Federal Institute of Technology, ETH Zurich,
Sonneggstrasse 3, CH-8092 Zürich, Switzerland

*corresponding author: pratsinis@ptl.mavt.ethz.ch

ABSTRACT

Agglomerates of particles arise from many natural and man-made processes. The structure and properties of these agglomerates remain an active research field especially with respect to their technical performance, possible health effects and environmental impact. Significant advances have been made in characterization of agglomerates (physically –bonded particles) by employing fractal theory and relating agglomerate structure to its generation pattern through the fractal dimension, D_f . Almost all studies focused on agglomerates of *monodisperse* primary particles. For coagulating aerosols, however, this needs to be carefully examined as Brownian coagulation leads to polydisperse particles. The effect of primary particle polydispersity on agglomerate structure is investigated here. A broader primary particle size distribution decreases D_f which becomes even independent of collision mechanism for sufficiently broad distributions ($\sigma_g > 2.5$). The anisotropy increases with increasing polydispersity.

Keywords: agglomerates, anisotropy, primary particle size distribution, fractal dimension, projected area exponent.

1 INTRODUCTION

Agglomeration is encountered in many natural or industrial processes, like growth of aerosol particles in the atmosphere, material synthesis by aerosol processes or even flocculation of minerals in oceans or colloidal particles. These particles collide by different mechanisms and stick together forming irregular or fractal-like agglomerates. The agglomeration of particles has been studied for over a century, but the focus has initially been on the kinetics of agglomeration rather than on their structure [1]. Medalia [2] was the first who characterized agglomerates made by ballistic particle-cluster agglomeration (BPCA) by a power law scaling between projected agglomerate area and primary particle (PP) number. Until then, there have been no comprehensive methods to study such complex and random structures. Forrest and Witten [3] introduced concepts of fractal-geometry to particle agglomeration and applied fractal analysis to smoke particles to encounter an “anomalous” power, because the exponent was not a simple fraction from dimensional consideration, the so-called fractal dimension D_f . Since then the concept of fractal-like agglomerates has been intensively studied [4, 5] for the

agglomeration of monodisperse primary particles. This concept has served well a wide spectrum of aerosol-made particles, in particular by coagulation. In fact, a number of characterization techniques and process design concepts have been developed capitalizing on these D_f values to extract other particle properties (e.g. collision diameter, primary particle size) and design reactors for manufacturing such particles.

In practical systems, however, the primary particles have almost always a size distribution. For example, primary particles grown by Brownian coagulation and full coalescence upon collision obtain a self-preserving size distribution (SPSD) with a standard deviation of $\sigma_g = 1.45$ in the free molecular [6] and continuum regime [7]. Figure 1 shows a zirconia agglomerate generated by scalable flame spray pyrolysis having $\sigma_g = 1.45$. What might have been overlooked in characterization and simulations of such particles is that the above D_f values have been developed for agglomerates of monodisperse primary particles. Exceptions are Tence et al. [8] and Bushell & Amal [9] who examined the effect of primary particle polydispersity on the agglomerate structure and their scattering behavior. They generated ballistic and diffusion-limited cluster-cluster agglomerates of Gaussian-distributed [8] and of mono-, bi- and tridisperse primary particles [9] and found no effect on D_f for their investigated polydispersities.

Here, the effect of PP polydispersity on D_f and projected area exponent D_a is investigated with agglomerates consisting of 16 – 1024 PP with closely controlled size distribution (geometric standard deviation, $\sigma_g = 1-3$, Figure 2). These simulations are in excellent agreement with the classic structure (D_f and prefactor k_n) of agglomerates consisting of monodisperse PPs made by four different collision mechanisms as well as with agglomerates of bi-, tri-disperse [9] and normally distributed PPs [8]. Broadening the PP size distribution of agglomerates decreases monotonically their D_f and for sufficiently broad PP distributions ($\sigma_g > 2.5$) the D_f reaches about 1.5 and k_n about 1 regardless of collision mechanism [10]. So the PP polydispersity determines for $\sigma_g > 2.5$ the agglomerate structure rather than the collision mechanism. So D_f can be an indication for PP polydispersity in mass–mobility and light scattering measurements, if the dominant agglomeration mechanism is known, like diffusion-limited and/or ballistic cluster-cluster coagulation in aerosols. Furthermore the effect of PP polydispersity on agglomerate anisotropy is studied.

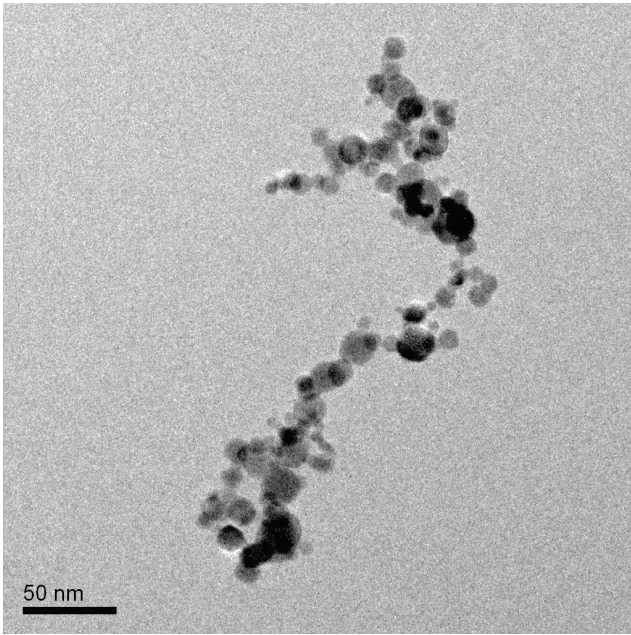


Figure 1: Zirconia agglomerate with a mobility radius $r_m = 75$ nm having a primary particle size distribution with $\sigma_g = 1.45$ generated by scalable flame spray pyrolysis.

2 THEORY

2.1 Agglomerate Generation

Agglomerates are generated numerically by diffusion-limited [DLA, 4] particle-cluster and cluster-cluster agglomeration [DLCA, 5] as well as ballistic particle-cluster [BPCA, 11] and cluster-cluster [BCCA, 8] agglomeration. One hundred agglomerates of each PP number ($n_p = 16-1024$) and mechanism are produced with log-normal PP diameter distributions having $\sigma_g = 1-3$. Figure 2 shows the PP diameter distributions for $\sigma_g = 1.45$ (circles, close to SPSP of Brownian coagulation), 2 (triangles) and 3 (squares).

2.2 Agglomerate Characterization

Fry et al. [12] used the moment of inertia tensor, \mathbf{T} , to describe the shape of fractal agglomerates:

$$\mathbf{T} = \sum_{i=1}^{n_p} v_{p,i} \begin{pmatrix} y_i^2 + z_i^2 & -x_i y_i & -x_i z_i \\ -x_i y_i & x_i^2 + z_i^2 & -y_i z_i \\ -x_i z_i & -y_i z_i & x_i^2 + y_i^2 \end{pmatrix} \quad (1)$$

where v_p is the volume of primary particle i and x , y and z are the distances between PP center and agglomerate center of mass. The eigenvalues of \mathbf{T} correspond to the square of principal radii of gyration r_j^2 for $j = 1-3$ and can

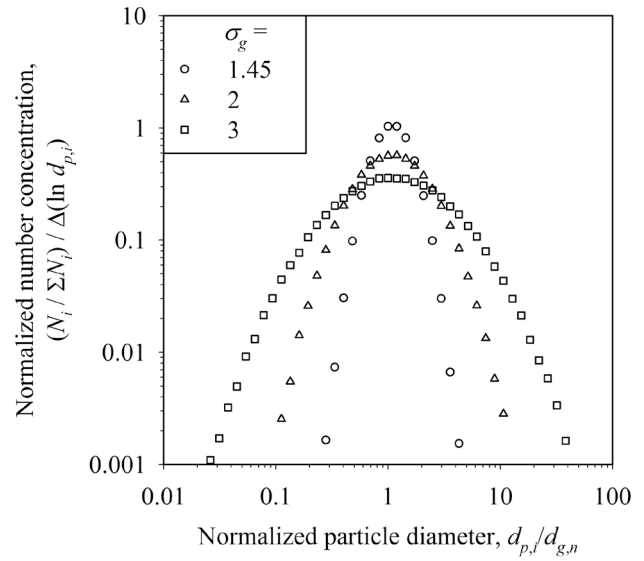


Figure 2: The log-normal primary particle diameter distributions with $\sigma_g = 1.45$ (circles), 2 (triangles) and 3 (squares).

be obtained by diagonalizing \mathbf{T} . The anisotropy is defined analogous to Botet and Jullien [13] as the ratio of the squares of the principal radii:

$$A_{ij} = \frac{r_i^2}{r_j^2} \quad (2)$$

with $r_i > r_j$. Here, the ratio between the largest and smallest principal radii r_1^2/r_3^2 is investigated. For a perfectly symmetric body $A_{ij} = 1$. The radius of gyration is:

$$r_g^2 = \frac{1}{2} (r_1^2 + r_2^2 + r_3^2) = \frac{\sum_i (x_i^2 + y_i^2 + z_i^2) m_i}{\sum_i m_i} \quad (3)$$

where m is the PP mass. The r_g exhibits a power law scaling with the number of primary particles n_p [3]:

$$n_p = k_n \left(\frac{r_g}{r_p} \right)^{D_f} \quad (4)$$

where D_f is the mass fractal dimension and k_n a constant prefactor. Also the rotationally averaged projected area, a_a , follows a power law scaling [2]:

$$n_p = k_a \left(\frac{a_a}{a_p} \right)^{D_a} = k_a \left(\frac{r_m}{r_p} \right)^{2D_a} \quad (5)$$

where D_α is the projected area exponent, k_a is again a constant prefactor and a_p is the primary particle projected area. The a_a is proportional to the mobility radius, r_m , in the free molecular regime: $a_a = \pi r_m^2$. Figure 3 shows a DLCA agglomerate with $n_p = 512$ and the radius of a sphere with equivalent moment of inertia (r_g , dashed line) and mobility (r_m , solid line).

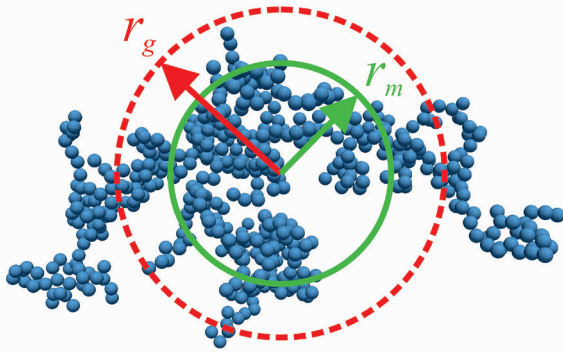


Figure 3: The radius of gyration, r_g , and mobility radius, r_m , of a diffusion-limited cluster-cluster agglomerate (DLCA) having 512 primary particles.

3 RESULTS & DISCUSSION

The agglomerates of monodisperse primary particles made by DLCA ($D_f = 1.79 \pm 0.03$) and BCCA ($D_f = 1.89 \pm 0.03$) have D_f values in excellent agreement with Botet et al. [5] and Tence et al. [8]. The D_f of DLA ($D_f = 2.25 \pm 0.02$) and BPCA ($D_f = 2.81 \pm 0.03$) are slightly smaller than their asymptotic limits of 2.5 and 3 by Witten and Sander [4] and Sutherland [11], respectively. This is a finite size effect, as the D_f of small agglomerates is always lower than their asymptotic D_f [11]. Table 1 summarizes the simulated

D_f values for $\sigma_g = 1, 2$ and 3. Polydisperse primary particles ($\sigma_g > 2$) result in more open asymptotic agglomerate structures decreasing D_f (Figure 4). This is most notable for particle-cluster (up to 50%) and to a lesser extent for cluster-cluster (up to 20%) ballistic and diffusion-limited collisions.

Table 1: Summary of the mass fractal dimension, D_f , of numerically generated agglomerates having primary particle size distributions with $\sigma_g = 1, 2$ and 3.

σ_g	D_f		
	1	2	3
DLCA	1.79	1.68	1.48
BCCA	1.89	1.74	1.52
DLA	2.25	1.91	1.51
BPCA	2.81	2.12	1.57

The projected surface area a_a of agglomerates determines mass, momentum and heat transfer of agglomerates in the free molecular and transition regime. Also D_α decreases with increasing polydispersity (Table 2) for all collision mechanisms.

Table 2: The projected area exponent, D_α , of agglomerates made by different collision mechanisms.

σ_g	D_α		
	1	2	3
DLCA	1.07	0.99	0.81
BCCA	1.09	1.01	0.86
DLA	1.11	1.03	0.83
BPCA	1.22	1.09	0.88

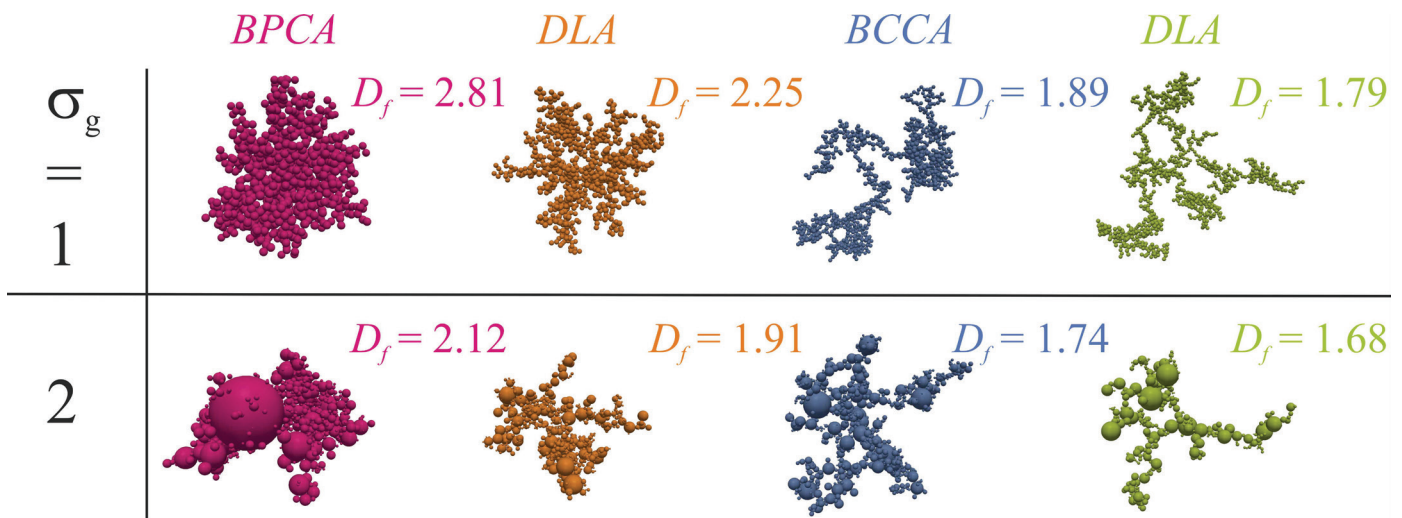


Figure 4: Agglomerates of monodisperse ($\sigma_g = 1$, top row) and polydisperse primary particles ($\sigma_g = 2$, bottom row) made by ballistic (BPCA) and diffusion-limited particle-cluster agglomeration (DLA) as well as by ballistic (BCCA) and diffusion-limited cluster-cluster agglomeration (DLCA).

Heinson et al. [14] showed by off-lattice DLCA Monte-Carlo (MC) simulations that the prefactor, k_n (eq. 4), correlates with the agglomerate anisotropy. Agglomerates with higher symmetry (lower A_{ij}) have a higher prefactor (e.g. $k_n = 1.83$) while stringier (chain-like) ones have a lower prefactor (e.g. $k_n = 0.95$) for the same D_f . The median agglomerate anisotropy A_{13} is shown in Fig. 5. The median is used instead of the mean as the anisotropy distribution has an exponential tail [12]. For monodisperse primary particles ($\sigma_g = 1$), the most compact and symmetric agglomerates (BPCA, $A_{13} = 1.61$) have the lowest $k_n = 0.46$ [10], which might be contradictory to Heinson et al. [14]. So the prefactor can be related best to the anisotropy within an ensemble of agglomerates made by the same collision mechanism and polydispersity, but probably not between agglomerates of different D_f . For example, A_{13} of DLCA particles is almost constant for $\sigma_g = 1$ -1.5 and increases with broader PPs size distribution to about 4.8. So the DLCA agglomerates are the most asymmetric of the four collision mechanisms with increasing σ_g , but still have a decreasing prefactor with increasing σ_g , similar to BCCA [10: Fig. 4b]. The DLA and BPCA particles, however, become progressively stringier for broader PP size distributions. Nevertheless their k_n increases to about 0.8 at $\sigma_g = 3$ [10: Fig. 4b]. The prefactor and anisotropy are related best within an ensemble of agglomerates of the same D_f as mentioned above. Drawing a conclusion about agglomerate structure (anisotropy) from k_n of agglomerates having different D_f is not possible at every σ_g , but works well within ensembles of agglomerates of the same collision mechanism and polydispersity [14].

4 CONCLUSIONS

Fractal-like agglomerates consisting of polydisperse primary particles were generated by DLCA, BCCA, DLA and BPCA having 16 – 1024 primary particles. The effect of log-normally distributed primary particle diameters on fractal dimension D_f and prefactor k_n , projected area exponent D_α and agglomerate anisotropy A_{13} are investigated. Asymptotic values of D_f and D_α are calculated for the geometric standard deviation σ_g ranging from 1.0 (monodisperse, consistent with literature) to 3.0. Increasing σ_g results in more open structures and thus decreases both D_f and D_α . As the agglomerates become stringier with increasing σ_g , their anisotropy increases. However, it is shown that the prefactor k_n can only be related to agglomerate anisotropy within an ensemble of agglomerates generated by the same collision mechanism.

REFERENCES

- [1] P. Meakin, J. Sol-Gel Sci. Technol. 15, 97 – 117, 1999.
- [2] A.I. Medalia, J. Colloid Interface Sci. 24, 393 – 404, 1967.
- [3] S.R. Forrest, T.A. Witten, J. Phys. A 12, L109 – L117, 1979.
- [4] T.A. Witten, L.M. Sander, Phys. Rev. Lett. 47, 1400-1403, 1981.
- [5] R. Botet, R. Jullien, M. Kolb, J. Phys. A 17, L75-L79, 1984.
- [6] S.C. Graham, A. Robinson, J. Aerosol Sci. 7, 261-273, 1976.
- [7] S.K. Friedlander, C.S. Wang, J. Colloid Interface Sci. 22, 126-132, 1966.
- [8] M. Tence, J.P. Chevalier, R. Jullien, J. Phys. 47, 1989 - 1998, 1986.
- [9] G. Bushell, R. Amal, J. Colloid Interface Sci. 205, 459 - 469, 1998.
- [10] M.L. Eggersdorfer, S.E. Pratsinis, Aerosol Sci. Technol. 46, 347 - 353, 2012.
- [11] D.N. Sutherland, J. Colloid Interface Sci. 22, 300-302, 1966.
- [12] D. Fry, A. Mohammad, A. Chakrabarti, C.M. Sorensen, Langmuir 20, 7871-7879, 2004.
- [13] R. Botet, R. Jullien, J. Phys. A 19, L907-L912, 1986.
- [14] W.R. Heinson, C.M. Sorensen, A. Chakrabarti, Aerosol Sci. Technol. 44, I-IV, 2010.

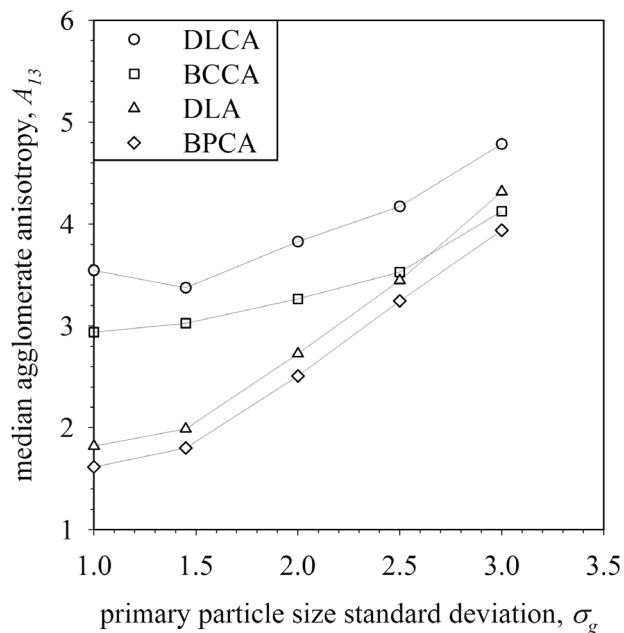


Figure 5: The median agglomerate anisotropy, A_{13} , increases with broader PP size distributions. A perfectly symmetric body has $A_{13} = 1$.